Self-attracting walk on heterogeneous networks

Kanghun Kim, Jaegu Kyoung, and D.-S. Lee*
Department of Physics, Inha University, Incheon 402-751, Korea
(Received 12 December 2015; revised manuscript received 14 April 2016; published 25 May 2016)

Understanding human mobility in cyberspace becomes increasingly important in this information era. While human mobility, memory-dependent and subdiffusive, is well understood in Euclidean space, it remains elusive in random heterogeneous networks like the World Wide Web. Here we study the diffusion characteristics of self-attracting walks, in which a walker is more likely to move to the locations visited previously than to unvisited ones, on scale-free networks. Under strong attraction, the number of distinct visited nodes grows linearly in time with larger coefficients in more heterogeneous networks. More interestingly, crossovers to sublinear growths occur in strongly heterogeneous networks. To understand these phenomena, we investigate the characteristic volumes and topology of the cluster of visited nodes and find that the reinforced attraction to hubs results in expediting exploration first but delaying later, as characterized by the scaling exponents that we derive. Our findings and analysis method can be useful for understanding various diffusion processes mediated by human.

DOI: 10.1103/PhysRevE.93.052310

I. INTRODUCTION

Human mobility is a key ingredient for urban planning, communication system design, preventing disease spread, and many other various applications [1–7]. The large-scale data-sets of the moving trajectories of human individuals in real space [8–10] and cyberspace [11] reveal that human mobility is characterized by a much slower increase of the mean square distance [9] and of the number of distinct visited places [11,12] with time than in the conventional random walks [13–16]. The origin and mechanism of such slow diffusion have attracted much attention [11,12,17–23], and the preference for a visited place to a strange one has been shown to be underlying [11,12]. Empirically, the probability of visiting a new place $p_{\rm new}$ decreases with the number of visited places S as $p_{\rm new} \sim S^{-\lambda}$ with $\lambda > 0$, which turns out to be capable of reproducing various empirical scaling relations in human mobility [12].

The probability to visit a new place $p_{\rm new}$ therefore characterizes human mobility at a fundamental level, but its properties and the origin of its scaling behavior are largely unknown. Here we investigate $p_{\rm new}$ in the self-attracting walk [24–30], a variant of the random walk modified toward incorporating the preference for places visited in the past, and show that the scaling exponent λ can vary with the heterogeneity of the substrate network. Our study is of particular relevance to human mobility in cyberspace, such as the World Wide Web (WWW) and online social media, which people spend increasingly longer time in and exhibit highly heterogeneous connectivity patterns, characterized by a large number of hubs as lots of macroscopic complex systems do [31–35]. Like in real space, the number of distinct browsed webpages S has been shown to increase sublinearly with time (the number of jumps) t as $S \sim t^{\nu}$ with $\nu < 1$ [11].

The behaviors of $p_{\rm new}(S)$ or $S(t)$, related to each other simply by $\frac{dS}{dt} = p_{\rm new}$, are studied in this paper, which enable one to understand the nature of diffusion under the influence of both memory and the substrate's heterogeneity. Especially, we focus on the case of strong attraction to visited places, which makes the walker's motion recurrent without regard to the dimensionality of substrates: the walker returns repeatedly to visited nodes. Then, on a heterogeneous substrate, the nodes having many neighbors (called hubs) can give the walker a higher chance to visit an unvisited node than those having few neighbors, especially in the early-time regime. Accordingly, $p_{\rm new}$ can be larger when the walker visits a hub than a nonhub, which brings the variation of $p_{\rm new}$ with the heterogeneity of the substrate. In the late-time regime, nonhub nodes remain to be visited and as a result, $S(t)$ can grow sublinearly with t, which is analyzed by investigating characteristic link-based volumes of the cluster of visited nodes. We discuss various structural characteristics of the substrate network, which can affect mobility under such self-attraction.

This paper is organized as follows. In Sec. II we introduce the self-attracting walk model and present simulation results on random scale-free (SF) networks. In Sec. III we show that $p_{\rm new}(S)$ in the strong self-attraction regime can be evaluated in terms of two characteristic volumes of the cluster of visited nodes, which are derived analytically in Sec. IV. Using the obtained results, we present asymptotic behaviors of $S(t)$ in Sec. V. The topology of the visited-node cluster with and without self-attraction is studied in Sec. VI. Finally we summarize and discuss our results in Sec. VII.

II. SELF-ATTRACTING WALK MODEL AND SIMULATION RESULTS

In the self-attracting walk (SATW) [24–30], a walker remembers all the locations visited previously and prefers to revisit them. Let us consider the SATW on a network and suppose that the walker is at a node i having k_i neighbors, among which only $\hat{k}_i$ have been visited and the remaining $k_i - \hat{k}_i$ not. The probability to hop from node i to a neighbor node j is given by (see Fig. 1)

$$w_{i\to j} = \begin{cases} w_i^{(\rm old)} = \frac{e^u}{k_i - \hat{k}_i + e^u \hat{k}_i} & (j \text{ visited}), \\ w_i^{(\rm new)} = \frac{1}{k_i - \hat{k}_i + e^u \hat{k}_i} & (j \text{ never visited}), \end{cases} \quad (1)$$

*deoksun.lee@inha.ac.kr

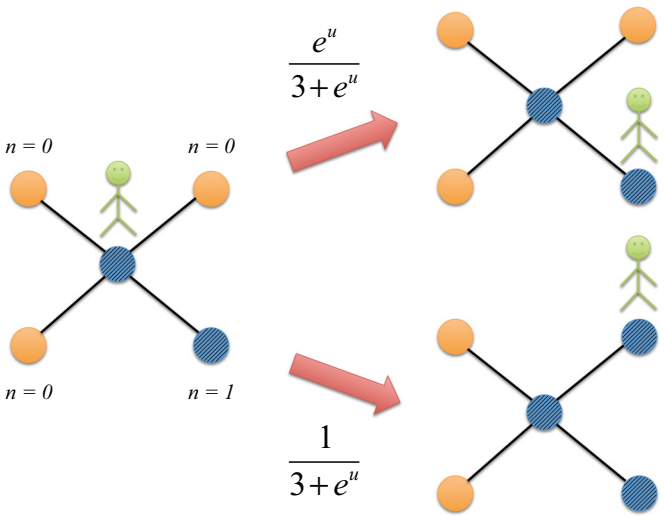

FIG. 1. Example of the transition probabilities in Eq. (1) of the SATW. Nodes with $n = 1$ ($n = 0$) are visited (unvisited) ones.

with $u > 0$ representing the self-attraction strength to the visited nodes. It is not the number of visits to a node but whether it was visited before or not that is stored in the walker's memory [12,19,20]. When $u = 0$, this model is reduced to the conventional random walk (RW) of $w_{i\to j} = w_i^{(\mathrm{new})} = w_i^{(\mathrm{old})} = 1/k_i$.

The mean number $S(t)$ of distinct visited nodes up to time (step) t can characterize the efficiencies of information searching or spreading, chemical reactions, and food forages [13–16,36,37]. In the SATW, S evolves with time in a stochastic way as

$$\frac{dS}{dt} = p_{\mathrm{new}}(S) = \sum_i (k_i - \hat{k}_i) w_i^{(\mathrm{new})} q_i, \tag{2}$$

where q_i is the probability for the walker to be at node i and $(k_i - \hat{k}_i)\, w_i^{(\mathrm{new})}$ is the probability to hop to any of its unvisited neighbors for given S. For $u \leqslant 0$, $p_{\mathrm{new}}(S)$ remains nearly unchanged in a wide range of S, giving $S \sim t$ [13,36].

In the complete graph of N nodes that are connected all-to-all, $k_i = N - 1$ for all i and $\hat{k}_i = S - 1$ for all visited nodes i. Therefore, $\omega_i^{(\mathrm{new})} = \frac{1}{N-S+(S-1)e^u}$ from Eq. (1), and Eq. (2) for S is read as

$$\frac{dS}{dt} = \frac{N - S}{N - S + (S-1)e^u}. \tag{3}$$

While this can be integrated to obtain $t = t(S)$, the asymptotic behaviors of $S(t)$ can be easily understood by examining Eq. (3), which depends on the competition between $N - S$ and $(S - 1)e^u$ in the denominator. One finds that $S(t)$ may display a crossover from $S \simeq t$ for $1 \ll t \ll t_c \equiv 2Ne^{-u}$ to $S \simeq \sqrt{2Nt/e^u}$ for $t \gg t_c$ if the self-attraction strength u satisfies $1 \ll e^u \ll N$. In the case of weak self-attraction, $e^u \sim 1$, the linear growth $S(t) \simeq t$ persists until the walker visits most nodes. On the other hand, under strong self-attraction, $e^u \gg N$, only the square-root growth is observed. In this case, p_{new} is given by the ratio of the number of unvisited nodes to that of visited ones,

$$p_{\mathrm{new}}(S) \simeq \frac{N - S}{e^u(S - 1)}, \tag{4}$$

divided by the factor e^u.

Also in the d-dimensional lattices, the growth of S can be delayed under strong self-attraction such that $S \sim t^\nu$ with $\nu < 1$ depending on the dimension d [27–30]. The origin of such sublinear growth has been explained as follows [27,28]. Strong self-attraction makes the cluster G_t of all the visited nodes up to time t and the edges connecting them compact. Thus, S can increase at $t + 1$ only when the walker is at a boundary node of G_t, linked to unvisited nodes. Consequently, $\frac{dS}{dt}$, or p_{new}, becomes proportional to the ratio of the area B of the boundary to the volume S of G_t, i.e., $dS/dt \sim B/S \sim S^{-1/d}$, where the last relation holds as the visited-node cluster is compact, leading to $S \sim t^{d/(d+1)}$. On the other hand, the diffusive behavior $\nu = 1$ appears under zero or weak self-attraction. Therefore, the distinction between the weak and the strong attraction regime and the question on the presence of a critical strength u_c on d-dimensional lattices has attracted great attention [25–29].

The architecture of real-world systems are far from complete graphs or regular lattices but display heterogeneous connectivity patterns characterized by power-law degree distributions $P_{\mathrm{deg}}(k) \sim k^{-\gamma}$ for $k \gg 1$ with degree k denoting the number of neighbors of a node and γ the degree exponent [31–35]. Our study is focused on the SATW on random SF networks having such a power-law degree distribution. Many random networks have an infinite fractal dimension $d_{\mathrm{f}} \to \infty$ and applying the above argument under the assumption that the cluster of visited nodes is compact, one could naively expect under strong attraction a linear growth $S \sim t^{d_{\mathrm{f}}/(d_{\mathrm{f}}+1)} \to t$.

Yet the compact growth of the visited-node cluster on random networks needs further investigation and so does the above conjecture. Constructing random SF networks with the configuration model [34,38,39], we perform simulations of the SATW on them with the self-attraction strength $u = 0$ and u=9 and find that $S(t)$ exhibits more complicated behaviors in the case of strong self-attraction $u = 9$ than expected as shown in Fig. 2(a). In the absence of self-attraction ($u = 0$), $S(t) \simeq t$ independent of γ. In contrast, with the strong self-attraction ($u = 9$), $S(t)$ is linear in t with the coefficient larger for smaller degree exponent γ in the early-time regime [Fig. 2(b)]. More interestingly, in the late-time regime, a sublinear growth of S appears, $S \sim t^\nu$ with the scaling exponent ν varying with γ for $\gamma < 3$ [Fig. 2(c)]. We observe quite similar behaviors of $S(t)$ for other sufficiently large u (see Appendix A) and investigate their origins in the following sections.

III. $p_{\mathrm{new}}(S)$ IN THE STRONG ATTRACTION REGIME

To understand complicated time and γ-dependent behaviors of S for large u shown in Fig. 2, we analyze Eq. (2). With u large enough,

$$w_i^{(\mathrm{new})} \simeq \frac{1}{e^u \hat{k}_i} \ll w_i^{(\mathrm{old})} \simeq \frac{1}{\hat{k}_i}, \tag{5}$$

and thus it takes long for the visited cluster G_t to grow by the walker's visiting a new node. Then local stationarity is

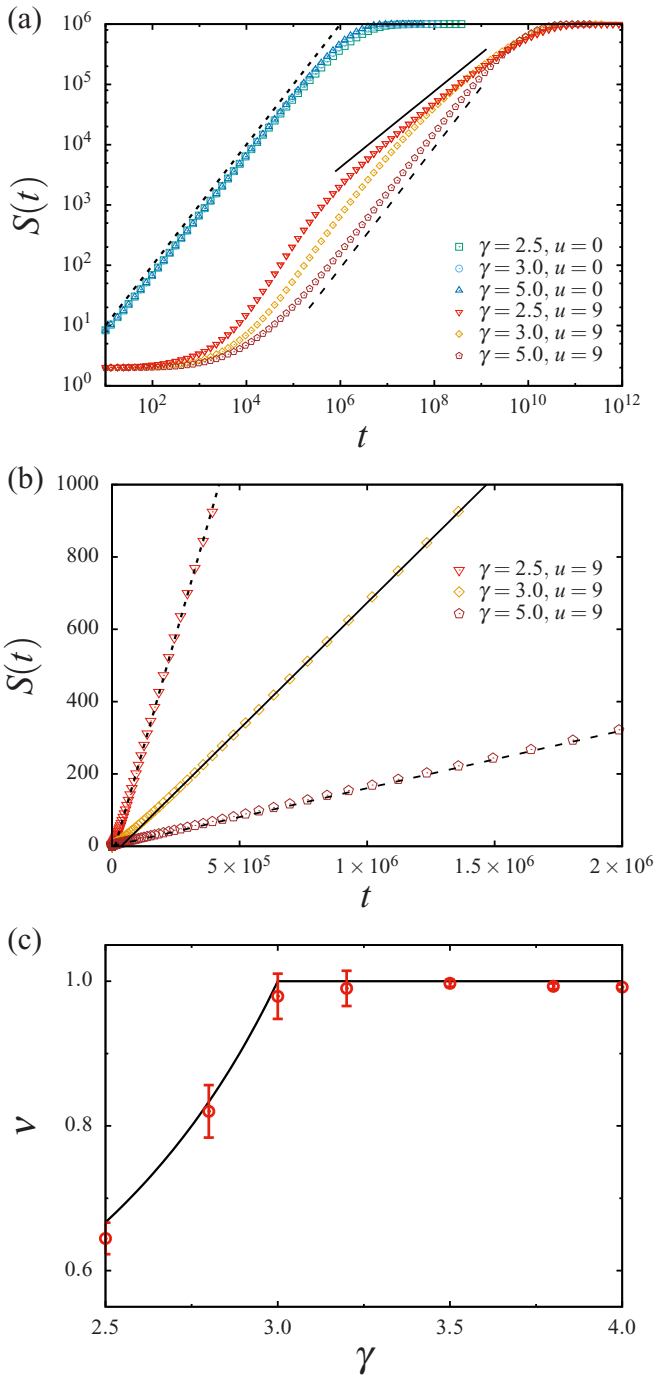

FIG. 2. (a) The mean number of distinct visited nodes S versus time step t for RW ($u = 0$) and SATW ($u = 9$) on uncorrelated SF networks of $N = 10^6$, $\langle k\rangle = 4$, and $\gamma = 2.5$, 3.0, and 5.0. Each data point is obtained by averaging over 1000 runs of simulation. The lines have slope 1 (dotted), 0.63 (solid), and 1 (dashed), respectively. (b) S versus t for SATW ($u = 9$) cropped in the early-time regime. All guidelines are linear and their coefficients are estimated as 24.5 (31.0), 6.98 (7.5), and 1.6 (1.58), all multiplied by 10^{-4}, for $\gamma = 2.5$, 3.0, and 5.0, respectively; the numbers in parentheses refer to the coefficients evaluated from Eqs. (17) and (18). (c) Estimated late-time scaling exponents ν in $S \sim t^{\nu}$ for $t \gg t_c$ for $\gamma < 3$ and for $t \gg 1$ otherwise, where t_c is given in Eq. (19). The line is from Eq. (20).

achieved such that the walker crosses every link of G_t with equal probability and accordingly the occupation probability q_i of node i becomes proportional to the number of its links belonging to G_t, i.e.,

$$q_i \simeq \frac{\hat{k}_i}{\hat{K}}, \tag{6}$$

where $\hat{K} = \sum_{i\in G_t} \hat{k}_i$ [40]. Using Eqs. (5) and (6) in Eq. (2), one finds

$$p_{\rm new}(S) \simeq \frac{K - \hat{K}}{e^u \hat{K}}, \tag{7}$$

where $K = \sum_{i\in G_t} k_i$. The validity of Eqs. (6) and (7) is checked against numerical simulations in Appendix B.

The expression for $p_{\rm new}$ in Eq. (7) under strong attraction is the generalization of Eq. (4) for the complete graphs and the argument for Euclidean lattices [27,28] to random networks. $\hat{K}$ is the sum of the number of visited neighbors $\hat{k}_i$, which we call the visited degree, of the visited nodes and K is the sum of their original full degrees k_i. While the links between visited nodes are counted in both $\hat{K}$ and K, the links between visited nodes and unvisited ones are counted only in K. Therefore, $K - \hat{K}$ can be considered as the link-based volume of the external boundary of G_t and $\hat{K}$ as the link volume of G_t itself.

IV. LINK-BASED VOLUMES OF THE CLUSTER OF VISITED NODES

Considering the order of visiting, one can represent K as

$$K(S) = \sum_{S'=1}^{S} \langle k_{\rm visit}(S')\rangle, \tag{8}$$

where $\langle k_{\rm visit}(S)\rangle$ is the expected degree of the Sth visited node. Since nodes of larger degrees are likely to be visited earlier, $\langle k_{\rm visit}(S)\rangle$ may decrease with S. In uncorrelated random networks, the $(S+1)$th visited node has degree k with probability $r_{S+1}(k) = kn(k|S)/\sum_{k'} k'n(k'|S)$, where $n(k|S)$ is the number of unvisited nodes of degree k for given S visited nodes and $n(k|0) = NP_{\rm deg}(k)$. Therefore, $\langle k_{\rm visit}(S)\rangle$ is evaluated as

$$\langle k_{\rm visit}(S)\rangle = \sum_k k\, r_S(k) = \sum_k k \frac{kn(k|S-1)}{\sum_{k'} k'n(k'|S-1)}. \tag{9}$$

If a node of degree k is indeed visited, $n(k|S+1)$ should be made smaller than $n(k|S)$ by one. Therefore, one finds a probabilistic relation $n(k|S) - n(k|S+1) = r_{S+1}(k) = kn(k|S)/\sum_{k'} k'n(k'|S)$ leading to

$$n(k|S) \sim k^{-\gamma} e^{-\frac{kS}{2L}}, \tag{10}$$

where L is the total number of links. The detailed procedures of derivation of Eq. (10) are given in Appendix C. The exponential factor represents the probability that a node of degree k remains unvisited when S nodes have been visited, $(1 - \frac{k}{2L})^S$ approximately, and imposes a constraint that the degree of the $(S+1)$th visited node is exponentially unlikely to be larger than the cutoff degree $k_c(S) = 2L/S$.

For $\gamma > 3$, the exponential factor in $n(k|S)$ makes little effect in Eq. (9) as the summands decay faster with k than

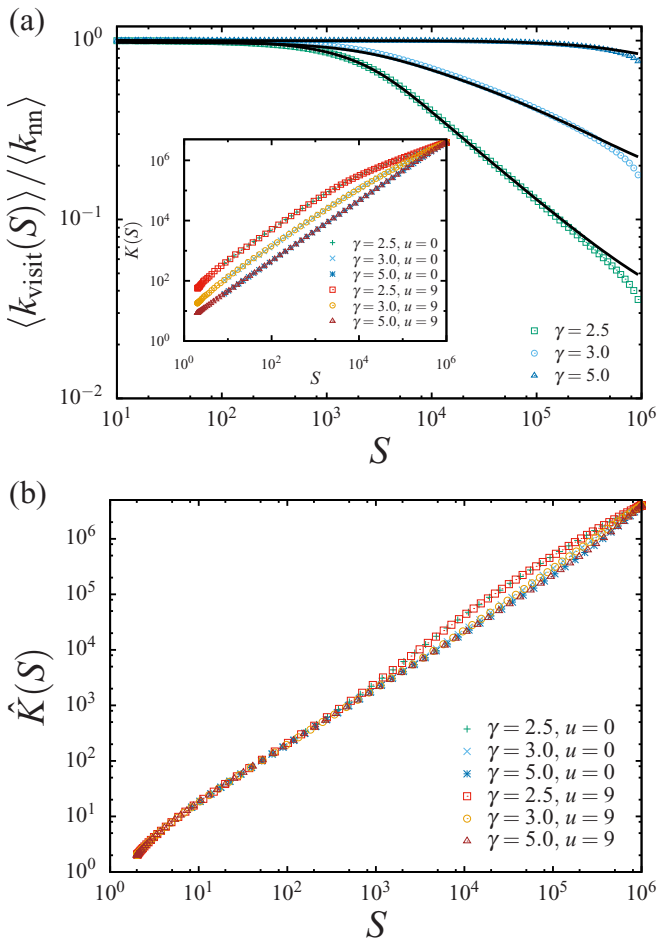

FIG. 3. (a) Degree of the Sth visited node $\langle k_{\rm visit}(S)\rangle$ for $N = 10^6$, $\langle k\rangle = 4$, $\gamma = 2.5$, 3.0, and 5.0. The lines are analytic results based on Eq. (13) and actually obtained from Eq. (C6), together with Eq. (C11) ($\gamma = 2.5$), Eq. (C14) ($\gamma = 3.0$), and Eq. (C10) ($\gamma = 5.0$), respectively. Inset: Sum of the degrees of visited nodes $K = \sum_{i\in G_t} k_i$ as a function of S. (b) Sum of the visited degrees of visited nodes $\hat{K} = \sum_{i\in G_t} \hat{k}_i$ as a function of S. For K and $\hat{K}$ in (a) and (b), no difference is seen between RW ($u = 0$) and SATW ($u = 9$).

k^{-1} such that the contributions from large k's are negligible. Therefore,

$$\langle k_{\rm visit}(S)\rangle \simeq \sum_k k \frac{kn(k|0)}{\sum_{k'} k' n(k'|0)} = \langle k_{\rm nn}\rangle, \tag{11}$$

where $\langle k_{\rm nn}\rangle \equiv \sum_k k^2 P_{\rm deg}(k) / \sum_k k P_{\rm deg}(k)$ is the mean degree of the nearest-neighbor nodes. It is shown in Fig. 3(a) that $\langle k_{\rm visit}(S)\rangle$ rarely decreases with S for $\gamma = 5.0$.

For $2 < \gamma < 3$, the sum in the numerator in Eq. (9) contains $k^{2-\gamma}$, decaying slower than k^{-1} and therefore the sum is governed by the contributions from large k's up to the smallest one among the largest degree k_M and the cutoff degree $k_c(S)$. Introducing a characteristic scale for S,

$$S_c \equiv \frac{2L}{k_M}, \tag{12}$$

TABLE I. Scaling behaviors of $K(S)$ dependent on the degree exponent γ with S_c in Eq. (12) and k_m the minimum degree. See Appendix C.

	$2 < \gamma < 3$	$\gamma = 3$	$\gamma > 3$
$S \ll S_c$	$\langle k_{\rm nn}\rangle S$		
$S \gg S_c$	$\frac{\Gamma(4-\gamma)}{\gamma-2}\langle k_{\rm nn}\rangle S_c \left(\frac{S}{S_c}\right)^{\gamma-2}$	$k_m S \ln \frac{2L}{S k_m}$	$\langle k_{\rm nn}\rangle S$

one finds that $k_c \ll k_M$ ($k_c \gg k_M$) for $S \gg S_c$ ($S \ll S_c$) and $\langle k_{\rm visit}(S)\rangle$ behaves as (see Appendix C)

$$\langle k_{\rm visit}(S)\rangle = \sum_k k \frac{kn(k|S-1)}{\sum_{k'} k' n(k'|S-1)} \simeq \begin{cases} \langle k_{\rm nn}\rangle & \text{for } S \ll S_c, \\ \Gamma(4-\gamma)\langle k_{\rm nn}\rangle \left(\frac{S}{S_c}\right)^{\gamma-3} & \text{for } S \gg S_c. \end{cases} \tag{13}$$

Figure 3(a) shows a good agreement between Eq. (13) and simulation results. $K(S)$ is obtained by using Eq. (13) in Eq. (8), the scaling behaviors of which are given in Table I.

Next we consider $\hat{K}$. Since the visited cluster G_t is connected, its number of links, $\hat{K}/2$, is not smaller than $S-1$ of tree structure, leading to $\hat{K} \geqslant 2(S-1)$. This lower bound is found to be a good approximation of $\hat{K}$ for sparse SF networks as long as $\gamma \geqslant 5/2$ due to its locally treelike structure [see Fig. 3(b)]:

$$\hat{K}(S) \simeq 2S. \tag{14}$$

To estimate the number of other links in G_t not counted in Eq. (14), we consider that two visited nodes i and j are connected by an additional link with probability $(k_i - 1)(k_j - 1)/2L$ [34,38], where it is used that one link for each node is included in Eq. (14). Hence, $\hat{K}(S)$ can be estimated as

$$\hat{K}(S) \simeq 2S + \frac{K(S)(K(S) - 2S)}{2L}. \tag{15}$$

Inserting the behaviors of $K(S)$ shown in Table I into Eq. (15), we find that for $2 < \gamma < 5/2$ the second term in Eq. (15) is dominant over the first one for $S \gg \hat{S}_c$ with another characteristic scale $\hat{S}_c$ given by

$$\hat{S}_c \equiv \frac{4L}{\langle k_{\rm nn}\rangle^2}. \tag{16}$$

As a result, for $2 < \gamma < 5/2$, $\hat{K}(S)$ shows crossovers twice at $\hat{S}_c$ and at S_c as in Table II.

We remark that $\langle k_{\rm visit}(S)\rangle$ is the same, given by Eq. (13), for both RW and SATW in uncorrelated random networks. As

TABLE II. Scaling behaviors of $\hat{K}(S)$ with b a constant larger than 2. See Appendix D.

	$2 < \gamma < 5/2$	$\gamma = 5/2$	$\gamma > 5/2$
$S \ll \hat{S}_c$	$2S$	$2S$	$2S$
$\hat{S}_c \ll S \ll S_c$	$\frac{\langle k_{\rm nn}\rangle^2}{2L} S^2$		
$S \gg S_c$	$\left(\frac{\Gamma(4-\gamma)}{\gamma-2}\langle k_{\rm nn}\rangle\right)^2 \frac{S_c^2}{2L}\left(\frac{S}{S_c}\right)^{2\gamma-4}$	$b\,S$	

K and $\hat{K}$ are determined by $\langle k_{\rm visit}(S)\rangle$, they are not different between RW and SATW either, as shown in Fig. 3.

V. SCALING OF THE NUMBER OF DISTINCT VISITED NODES

Using the scaling behaviors of $K(S)$ and $\hat{K}(S)$ in Tables I and II, respectively, in Eq. (7), we find in the SATW under strong attraction that for $\gamma \geqslant 3$,

$$S(t) \sim (\langle k_{\rm nn}\rangle/2-1)e^{-u}t, \tag{17}$$

for all t, and for $5/2 \leqslant \gamma < 3$,

$$S(t) \sim \begin{cases} (\langle k_{\rm nn}\rangle/2-1)e^{-u}t & \text{for } S \ll S_c, \\ S_c(t/t_c)^{1/(4-\gamma)} & \text{for } S \gg S_c, \end{cases} \tag{18}$$

with the characteristic time

$$t_c \equiv \frac{S_c e^u}{\langle k_{\rm nn}\rangle} = \frac{2L\,e^u}{k_M\langle k_{\rm nn}\rangle}. \tag{19}$$

These analytic results help us understand all the behaviors of S shown in simulations (Fig. 2), especially revealing the late-time scaling exponent

$$\nu = \min\{1, 1/(4-\gamma)\}. \tag{20}$$

S increases faster for $\langle k_{\rm nn}\rangle$ larger in the early-time regime as shown in Eqs. (17) and (18), which explains the larger coefficient of the linear growth of S in more heterogeneous networks under strong attraction, as shown in Fig. 2(b). Note that $\langle k_{\rm nn}\rangle \sim k_M^{3-\gamma}$ diverges with N for $\gamma < 3$ while $\langle k_{\rm nn}\rangle$ is finite for $\gamma > 3$. We remark that for $\gamma \leqslant 3$, $(\langle k_{\rm nn}\rangle/2-1)e^{-u}$ is a bit larger than the measured coefficients in Fig. 2(b) and that the simulation data of $S(t)$ increases slowly in the very early time regime, deviating from the linear growth. The origin of these deviations are not explained within the framework of our theoretical approach but need more investigations. The slow exploration in the late-time regime comes from the sublinear growth of $K \sim S^{\gamma-2}$ from Eq. (13) and Table I, which happens as most of hub nodes have been visited early in strongly heterogeneous networks with $\gamma < 3$. The crossover behavior of $S(t)$ shown in Eq. (18) is confirmed by the data collapse of the scaled data S/S_c versus t/t_c with different N's in Fig. 4.

In SF networks of $2 < \gamma < 5/2$, $S(t)$ is expected to undergo a crossover from t to $\sqrt{t}$ first around $\hat{S}_c$ and another crossover to $t^{1/(\gamma-1)}$ next around S_c. However, we could not observe these crossovers in our simulations under strong attraction with networks as large as of $N = 10^6$. It is probably due to the finite-size effects: Three distinct scalings are not wide enough. The simulation of the SATW with large u on bigger networks than $N = 10^6$ appears nearly unfeasible. On the other hand, the simulation with $u = 0$—equivalent to RW—is attainable even for very large networks. To estimate how $S(t)$ behaves under strong attraction for $2 < \gamma < 5/2$ in very large networks, we compute approximately $S(t)$ as follows. We first obtain numerically $K(S)$ and $\hat{K}(S)$ from the simulation with $u = 0$. $K(S)$ and $\hat{K}(S)$ do not depend on u in uncorrelated networks as we showed in Fig. 3, and therefore we can insert them into the approximate expression of $p_{\rm new}(S)$ in Eq. (7) that we have shown valid for sufficiently large u. Using these numerical data of $p_{\rm new}(S)$ in the relation $\frac{dS}{dt} = p_{\rm new}(S)$ and integrating it with respect to time numerically, we can obtain $S(t)$ in the SATW with large u for very large networks. Figure 5 shows $S(t)$ estimated in that way for SF networks of $N = 10^9$, $\gamma = 2.2$, and large u, which seems to exhibit the expected consecutive crossovers. The scaling behaviors of $S(t)$ under strong attraction are summarized in Table III.

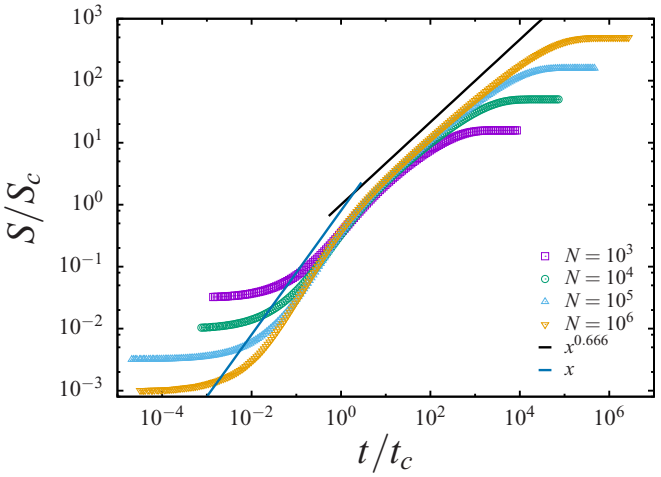

FIG. 4. Plots of S/S_c versus t/t_c for the SATW on uncorrelated SF networks with different system sizes and $\langle k\rangle = 4$, $\gamma = 2.5$. Here, $u = 7$ for $N = 10^3, 10^4$ and $u = 9$ for $N = 10^5, 10^6$, respectively. The crossover from a linear to a sub-linear growth is in good agreement with Eq. (18).

VI. TOPOLOGY OF THE VISITED CLUSTER

Comparing the topology of the visited cluster with and without self-attraction helps a deeper understanding of how the self-attraction and the topological heterogeneity of substrates affect the behavior of S. Without self-attraction (RW), the walker is likely to pass through a hub node without visiting all

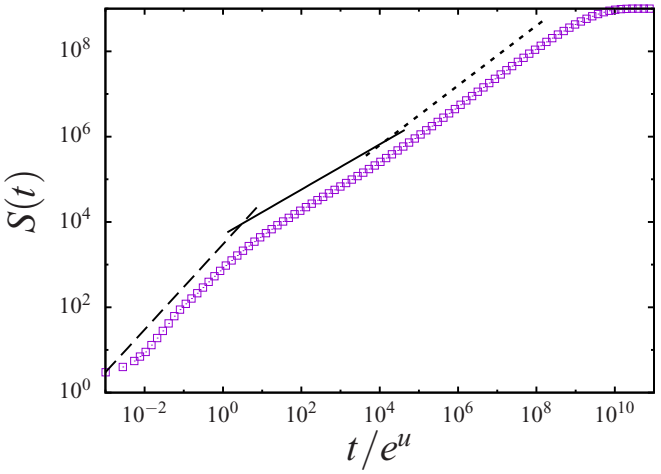

FIG. 5. $S(t)$ in SATW ($u = 12$) on uncorrelated SF networks of $N = 10^9$, $\langle k\rangle = 4$, and $\gamma = 2.2$, obtained indirectly by numerical integrations of $\frac{dS}{dt} = p_{\rm new}(S)$ with $p_{\rm new}(S)$ evaluated by K and $\hat{K}$ from RW ($u = 0$) simulations. The lines have slope 1 (dashed), 0.53 (solid), and 0.7 (dotted), respectively.

TABLE III. Scaling behaviors of $S(t)$ under strong attraction in the SATW. Here $\tau = t/e^u$, $A = \langle k_{\rm nn}\rangle/2 - 1$, $B = \sqrt{4L/\langle k_{\rm nn}\rangle}$, $C_1 = S_c\langle k_{\rm nn}\rangle^{1/(1-\gamma)}$, $C_2 = S_c(\langle k_{\rm nn}\rangle/S_c)^{1/(4-\gamma)}$, and $C_3 = k_m/2$.

	$2 < \gamma < 5/2$	$5/2 \leqslant \gamma < 3$	$\gamma = 3$	$\gamma > 3$
$S \ll \hat{S}_c$	$A\,\tau$	$A\,\tau$	$A\,\tau$	$A\,\tau$
$\hat{S}_c \ll S \ll S_c$	$B\,\sqrt{\tau}$			
$S \gg S_c$	$C_1\,\tau^{1/(\gamma-1)}$	$C_2\,\tau^{1/(4-\gamma)}$	$C_3\tau \ln \frac{L}{\tau}$	

of its neighbors, forming a chain-like visited cluster [Fig. 6(a)]. When encountering again the hub after visiting many other nodes, the walker would see many of its neighbors yet unvisited. On the other hand, with self-attraction (SATW), once visiting a hub node, the walker returns repeatedly to the hub. Since the hub has many unvisited neighbor nodes in the early-time regime, the walker has a higher chance to visit a new node there than at nonhub ones. Therefore, the cluster of visited nodes blooms at the visited hubs, leading the whole cluster to look like a union of starlike subgraphs [Fig. 6(b)]. Broader distributions of the visited degree $\hat{k}$ in Fig. 6(c) also exhibit such difference in visited clusters between RW and SATW.

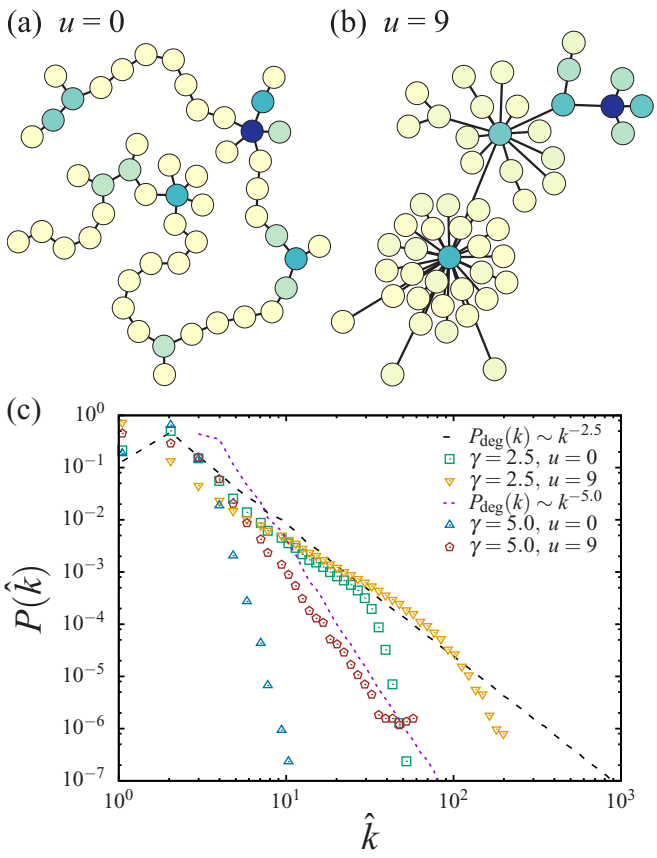

FIG. 6. Visited clusters for (a) RW and (b) SATW at $S = 50$ in an SF network of $N = 10^6$, $\langle k\rangle = 4$, and $\gamma = 2.5$. Darker colored nodes represent more frequently visited ones. (c) Distribution of the visited degree $\hat{k}$ at $S = 1280$ for RW and for SATW in SF networks with $\gamma = 2.5$ and 5.0, respectively. The original degree distributions $P_{\rm deg}(k)$ are drawn for comparison.

The larger volume of the boundary, due to more abundant hubs, results in the faster growth of S in the early-time regime. In the late-time regime, most hubs have been already visited and nodes with smaller degrees remain unvisited as shown in Eq. (13). This results in the slower growth of the boundary $K - \hat{K}$ than that of $\hat{K}$ of the cluster, leading to the decrease of $p_{\rm new}(S)$ with S and the sub-linear growth of S in strongly heterogeneous networks.

VII. SUMMARY AND DISCUSSION

As a minimal model for the human mobility patterns in inhomogeneous media, we considered the SATW on random SF networks and studied the scaling behaviors of the mean number of distinct visited nodes. We showed that under the considered type of attraction, dependent only on whether a node has been visited or not, the probability to visit a new node $p_{\rm new}(S)$ is simply represented in terms of two characteristic link-based volumes $K(S)$ and $\hat{K}(S)$ of the cluster of S visited nodes as long as the attraction strength is sufficiently large. The volumes of the visited cluster can be computed analytically in uncorrelated networks, which are used to derive $S(t)$. This study demonstrates that subdiffusive motion can arise in the presence of strong self-attraction and heterogeneity of substrates, and furthermore explains its origins in terms of the characteristics of the growth of the visited cluster.

The degree-degree correlation, which we assumed to be absent, can affect the behaviors of $S(t)$ and the volumes of the visited cluster. Under a positive degree-degree correlation, nodes with similar degrees are more likely to be connected than those with different degrees. Therefore, compared to uncorrelated networks, $K(S)$ and $\hat{K}(S)$ grow faster in first exploiting more abundant hub-hub connections but slower later due to the early exhaustion of unvisited hubs. These changes result in the faster increase of $S(t)$ in the early time and slower in the late time (Fig. 7). The opposite changes happen when a negative correlation is introduced.

In dense networks with $\langle k\rangle$ large, the visited cluster is no longer of tree structure: $\hat{K} \sim S^2$ in the complete graphs, in contrast to Eq. (14). It is shown in Fig. 8 that as $\langle k\rangle$ increases, the scaling behavior of $S(t)$ approaches $\sqrt{t}$ of complete graphs.

Our results for the SATW on random SF networks of $d_{\rm f} \to \infty$ and γ finite are complementary to the previous studies for the Euclidean lattices of $d_{\rm f}$ finite and $\gamma \to \infty$ [24–30]. Some real-world networks have both γ and $d_{\rm f}$ finite [42–46], demanding further studies.

While we had unveiled anomalous scalings of SATW under strong attraction, the robustness of our findings against the variation of the attraction strength u, the presence of a critical value u_c, and their dependence on the degree exponent γ remain still elusive, demanding more extensive and rigorous investigations. The effects of different kinds of memories are also of great interest [47–52].

This work can be used to investigate how the structural features of real-world infrastructure affect the efficiency of transportation of materials and information mediated by humans. The growth pattern of the visited cluster has proved to be useful in analyzing our model system. It can be investigated further for classifying and quantitatively analyzing the

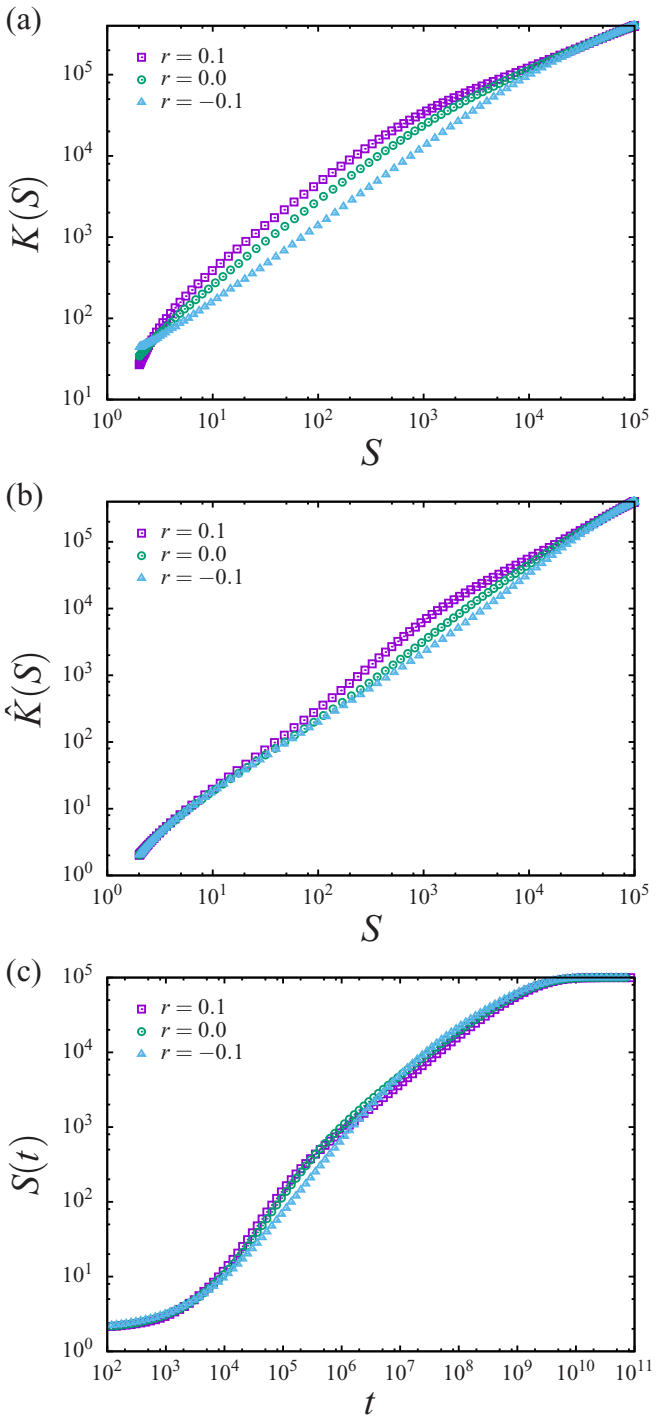

FIG. 7. SATW ($u = 9$) on SF networks with positive degree-degree correlation (assortativity coefficient $r = 0.1$), no correlation ($r = 0$), and negative correlation ($r = -0.1$) [41]. All network ensembles have the same degree sequence and $N = 10^5$, $\langle k \rangle = 4$, $\gamma = 2.5$.

behavior of human individuals online, e.g., browsing new pages in WWW [11] or visiting strangers' pages in social media, and the patterns of information and epidemic spreading, which can be of great use in online marketing, advertisement, cyber security, public health, and so on.

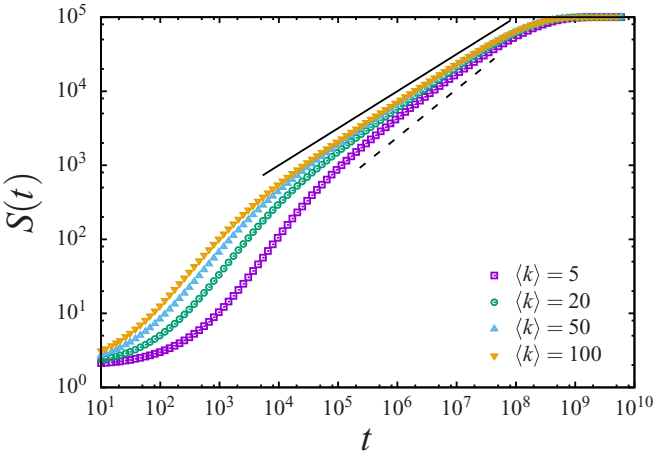

FIG. 8. $S(t)$ in the SATW ($u = 7$) on uncorrelated SF networks with $N = 10^5$, $\gamma = 2.5$, and different $\langle k \rangle$'s. As $\langle k \rangle$ grows, the scaling exponent of S in the late-time regime gradually decreases from 0.66 (dotted) to 0.5 (solid).

ACKNOWLEDGMENTS

We acknowledge J. W. Lee, B. Kahng, and S. Hwang for useful discussions and computing resources. This work was supported by the National Research Foundation of Korea (NRF) grants funded by the Korean Government (Grant No. 2013R1A2A2A01068845).

APPENDIX A: STRONG ATTRACTION REGIME

While in Fig. 2, $S(t)$ of the SATW is presented only for $u = 9$, the same functional behaviors of $S(t)$ are observed also for other sufficiently large u, suggesting the presence of the strong attraction regime in the SATW on SF networks. The effects of self-attraction strength u has been one of the most primary issues in the investigation of the SATW on the Euclidean lattices, including whether a phase transition occurs and if so, the accurate critical strength u_c [25–29]. Therefore, it would be desirable if we locate the boundary of the strong attraction regime and illuminate the nature of the boundary in the SATW on SF networks. Figure 9 shows the data collapse of $S(t)$ with $u = 7$, 9, 10 when plotted as a function of a scaled time t/e^u in SF networks with $\gamma = 2.5$, demonstrating the existence of a subdiffusive phase in SATW on SF networks, distinguished from the normal diffusive phase for $u = 0$ and small u. The fact that $S(t)$ is a function of t/e^u is consistent with Eq. (7) combined with our observation that K and $\hat{K}$ are not affected by the attraction in uncorrelated random networks, shown in Fig. 3. Our analytic approach for the strong attraction regime begins with the approximation in Eq. (5), which is valid if $e^u \gg k_{\max}$. It is a sufficient condition to satisfy Eq. (5), however, and the numerical data in Fig. 9 suggest the possibility that the subdiffusive phase exists even without satisfying $e^u \gg k_{\max}$. Therefore, the exact location and the nature of the boundary between the strong and the weak attraction regime on SF networks, including its dependence on the degree exponent γ and the mean connectivity $\langle k \rangle$, are beyond the scope of the present work, and demand further studies.

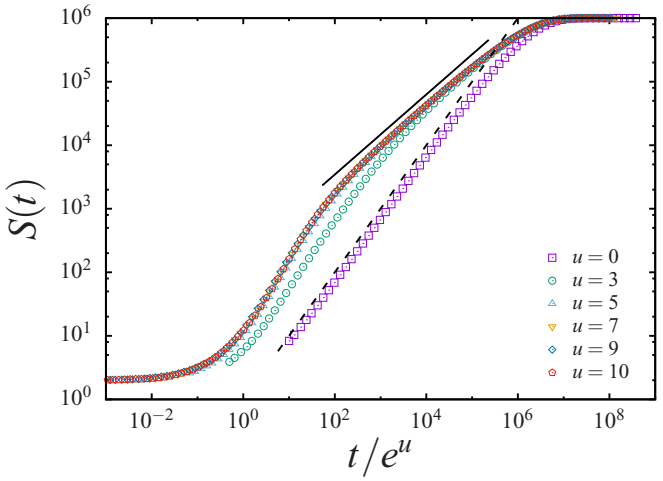

FIG. 9. S as a function of the scaled time t/e^u in the SATW with various self-attraction strengths u on uncorrelated SF networks with $N = 10^6$, $\langle k\rangle = 4$, and $\gamma = 2.5$. For $u = 7$, 9, 10, all $S(t)$ collapse perfectly to a single curve, displaying the sublinear behavior in the late-time regime. The guidelines have slope 0.63 (solid) and 1 (dashed), respectively.

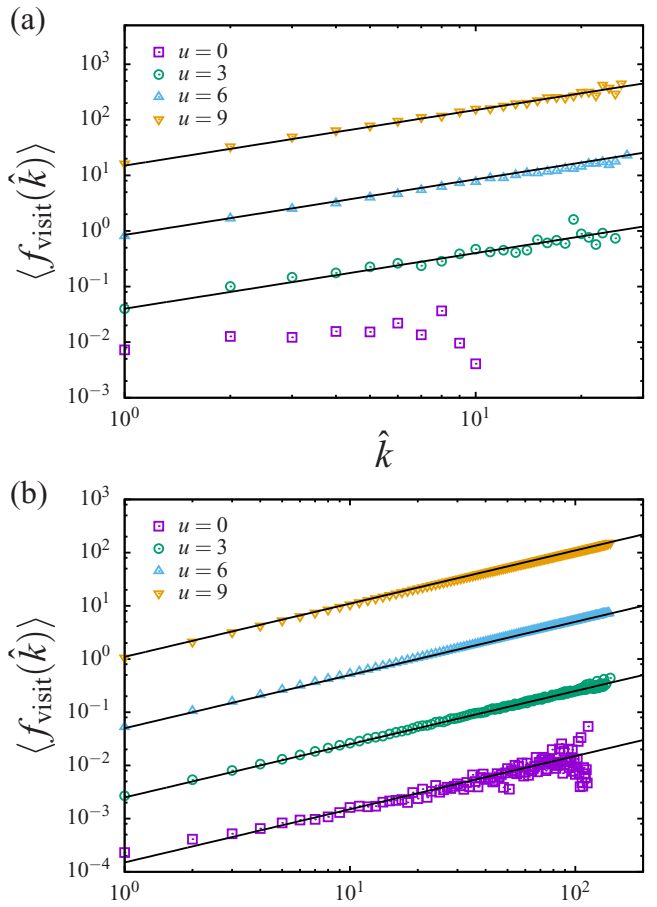

FIG. 10. The mean number of visits $\langle f_{\rm visit}\rangle$ versus visited degree $\hat{k}$ for various self-attraction strengths u measured at (a) $S = 40$ and (b) $S = 2560$ in the SATW on uncorrelated SF networks with $N = 10^4$, $\langle k\rangle = 4$, and $\gamma = 2.5$. The slope of all the solid lines is 1.

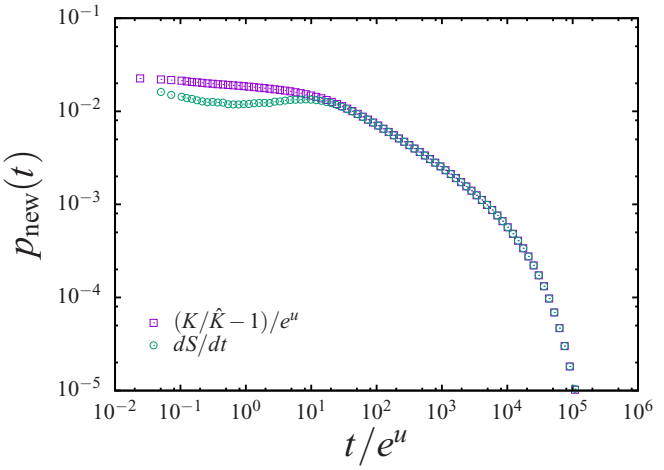

FIG. 11. $p_{\rm new}(t)$ in the SATW on uncorrelated SF networks with $N = 10^4$, $\langle k\rangle = 4$, $\gamma = 2.5$, and $u = 6$, estimated in two distinct ways. See the text in Appendix B.

APPENDIX B: VALIDITY OF EQS. (6) AND (7)

To examine Eq. (6), we obtained the mean number of visits $\langle f_{\rm visit}(\hat{k})\rangle$ of the nodes having visited degree $\hat{k}$ while $S(t)$ remains at a fixed value, say S, in simulations, which is expected to be proportional to $\hat{k}$ by Eq. (6). Figures 10(a) and 10(b) show that $\langle f_{\rm visit}(\hat{k})\rangle \propto \hat{k}$ for different S's and u's, supporting Eq. (6).

Next we estimate $p_{\rm new}$ in two distinct ways; one is to numerically differentiate $S(t)$ obtained from simulations, and the other is to use the righthand side of Eq. (7) with $K(S)$ and $\hat{K}(S)$ from simulations. Figure 11 shows that two results are in excellent agreement, supporting the validity of Eq. (7).

APPENDIX C: DERIVATION OF EQS. (10) AND (13)

In the uncorrelated SF networks constructed in this work, the degree distribution is given by $P(k) \sim k^{-\gamma}$ for $k \in [k_m, k_M]$ with $k_M \simeq \sqrt{\langle k\rangle N}$ for $2 < \gamma \leqslant 3$ and $k_M \simeq k_m N^{1/(\gamma-1)}$ for $\gamma > 3$ [39,53].

Let us denote the probability that the $(S+1)$th visited node has degree k by $r_{S+1}(k)$. Then $r_{S+1}(k)$ is proportional to the total number of links connected to all *unvisited* nodes of degree k, i.e., $kn(k|S)$, where $n(k|S)$ is the mean number of unvisited nodes of degree k after S nodes have been visited, and it is given by

$$r_{S+1}(k) = \frac{kn(k|S)}{2L(S)}, \tag{C1}$$

where $2L(S) = \sum_k kn(k|S) = 2L - K(S)$, the sum of degrees of $N - S$ unvisited nodes, in average. As the number of unvisited nodes of degree k decreases by 1 with probability $r_{S+1}(k)$, $n(k|S)$ satisfies a recursion relation

$$n(k|S) - n(k|S+1) = r_{S+1}(k) = \frac{kn(k|S)}{2L(S)}. \tag{C2}$$

As $k \ll 2L(S)$, Eq. (C2) gives

$$n(k|S) = n(k|0)\prod_{S'=0}^{S-1}\left[1 - \frac{k}{2L(S')}\right] \simeq NP(k)e^{-k/k_c(S)}, \tag{C3}$$

where the cutoff degree k_c is defined as

$$k_c^{-1}(S) = \sum_{S'=0}^{S-1} \frac{1}{2L(S')} = \sum_{S'=0}^{S-1} \frac{1}{2L - K(S')} = \sum_{S'=0}^{S-1} \frac{1}{2L - \sum_{i=1}^{S'} \langle k_{\rm visit}(i)\rangle}. \quad \text{(C4)}$$

Using Eq. (C2) in Eq. (9), we obtain

$$\langle k_{\rm visit}(S+1)\rangle = \frac{\sum_k k^2 n(k|S)}{\sum_k k n(k|S)} \simeq \frac{\sum_k k^{2-\gamma} e^{-k/k_c(S)}}{\sum_k k^{1-\gamma} e^{-k/k_c(S)}}. \quad \text{(C5)}$$

Equations (C4) and (C5) are coupled and can be solved in a self-consistent way. Using the continuum approximation replacing $\sum_k$ by $\int dk$, Eq. (C5) is represented as

$$\langle k_{\rm visit}(S)\rangle \simeq k_c \frac{\Gamma\left(3-\gamma, \frac{k_m}{k_c}\right) - \Gamma\left(3-\gamma, \frac{k_M}{k_c}\right)}{\Gamma\left(2-\gamma, \frac{k_m}{k_c}\right) - \Gamma\left(2-\gamma, \frac{k_M}{k_c}\right)}, \quad \text{(C6)}$$

where $\Gamma(a,x) \equiv \int_x^\infty t^{a-1} e^{-t} dt$ is the incomplete gamma function [54] and Eq. (C4) is reduced to

$$\frac{f''(S)}{[f'(S)]^2} \simeq \langle k_{\rm visit}(S)\rangle, \quad \text{(C7)}$$

where $f(S) \equiv k_c^{-1}(S)$. As k_c decreases with S, it is convenient to consider two regimes, $k_M \ll k_c(S)$ and $k_M \gg k_c(S)$. Introducing the crossover scale S_c in Eq. (12) with which $k_c(S_c) = k_M$, the regime of $k_M \ll k_c(S)$ corresponds to $S \ll S_c$ and that of $k_M \gg k_c(S)$ to $S \gg S_c$.

For $2 < \gamma < 3$, Eq. (C6) is approximated up to the leading order as

$$\langle k_{\rm visit}(S)\rangle \simeq \begin{cases} \frac{\gamma-2}{3-\gamma} k_m^{\gamma-2} k_M^{3-\gamma} & \text{for } S \ll S_c, \\ \frac{\gamma-2}{\Gamma^{-1}(3-\gamma)} k_m^{\gamma-2} k_c^{3-\gamma} & \text{for } S \gg S_c, \end{cases} \quad \text{(C8)}$$

where $\Gamma(a)$ is the gamma function [54]. Note that $\langle k_{\rm visit}(S)\rangle \simeq \langle k_{\rm nn}\rangle$ for $S \ll S_c$ since

$$\langle k_{\rm nn}\rangle \simeq \frac{\int_{k_m}^{k_M} dk k^{2-\gamma}}{\int_{k_m}^{k_M} dk k^{1-\gamma}} \simeq \frac{\gamma-2}{3-\gamma} k_m^{\gamma-2} k_M^{3-\gamma}. \quad \text{(C9)}$$

Equation (C8) indicates that $\langle k_{\rm visit}(S)\rangle$ remains nearly fixed at $\langle k_{\rm nn}\rangle$ for $S \ll S_c$ while diminishes for $S \gg S_c$. Solving Eq. (C7) with $\langle k_{\rm visit}\rangle = \langle k_{\rm nn}\rangle$ used, we obtain

$$k_c^{-1}(S) = \frac{1}{\langle k_{\rm nn}\rangle} \ln\left[\frac{2L}{2L - \langle k_{\rm nn}\rangle S}\right] \simeq \frac{S}{2L} + \frac{\langle k_{\rm nn}\rangle}{2}\left(\frac{S}{2L}\right)^2. \quad \text{(C10)}$$

With Eq. (C8) for $S \gg S_c$ and a trial solution $f(S) = S/2L + g(S)$ in Eq. (C7), we obtain

$$k_c^{-1}(S) \simeq \frac{S}{2L} + \frac{\Gamma(3-\gamma)}{\gamma-1} k_m^{\gamma-2}\left(\frac{S}{2L}\right)^{\gamma-1}. \quad \text{(C11)}$$

Equations (C10) and (C11) show that

$$k_c(S) \simeq \frac{2L}{S} \quad \text{(C12)}$$

for both $S \ll S_c$ and $S \gg S_c$, up to the leading order. Using Eq. (C12) in Eq. (C8), we obtain Eq. (13).

The asymptotic behaviors of $\langle k_{\rm visit}(S)\rangle$ for $\gamma = 3$ can be obtained similarly as

$$\langle k_{\rm visit}(S)\rangle \simeq \begin{cases} \langle k_{\rm nn}\rangle & \text{for } S \ll S_c, \\ k_m \ln \frac{2L}{k_m S} & \text{for } S \gg S_c, \end{cases} \quad \text{(C13)}$$

where $\langle k_{\rm nn}\rangle \simeq k_m \ln k_M / k_m$. For $S \gg S_c$, k_c is given by, up to the subleading term,

$$k_c^{-1}(S) \simeq \frac{S}{2L} + \frac{k_m}{2}\left(\frac{S}{2L}\right)^2 \ln \frac{2L}{k_m S}. \quad \text{(C14)}$$

APPENDIX D: DERIVATION OF THE SCALING BEHAVIORS OF $\hat{K}$ IN Table II

Inserting the behaviors of $K(S)$ in Table I into Eq. (15), one can obtain the scaling behaviors of $\hat{K}$. For $\gamma > 3$, $K \simeq \langle k_{\rm nn}\rangle S$ for all S and thus

$$\hat{K}(S) \simeq 2S + \frac{\langle k_{\rm nn}\rangle(\langle k_{\rm nn}\rangle - 2)}{2L} S^2. \quad \text{(D1)}$$

Given that $\langle k_{\rm nn}\rangle$ is finite for $\gamma > 3$, the second term is always dominated by the first term.

Next let us consider the case of $2 < \gamma < 3$. In the regime $S \ll S_c$, $K \simeq \langle k_{\rm nn}\rangle S$ and thus Eq. (D1) holds in this case. However, $\langle k_{\rm nn}\rangle$ is not finite in this case and the second term in Eq. (D1) can be dominant for $S \gg \hat{S}_c$ with $\hat{S}_c$ in Eq. (16) as

$$\hat{K}(S) \simeq \begin{cases} 2S & \text{for } S \ll \hat{S}_c, \\ \frac{\langle k_{\rm nn}\rangle^2}{2L} S^2 & \text{for } \hat{S}_c \ll S \ll S_c. \end{cases} \quad \text{(D2)}$$

As we consider the regime $S \ll S_c$, the quadratic behavior of $\hat{K}(S)$ can be indeed observed only if $\hat{S}_c \ll S_c$. The two characteristic scales are given by $S_c = 2L/k_M$ and $\hat{S}_c = 4L/\langle k_{\rm nn}\rangle^2 \simeq 4L/k_M^{2(3-\gamma)}$, respectively, and thus $\hat{S}_c$ is smaller than S_c only for $2 < \gamma < 5/2$.

For $S \gg S_c$ and $2 < \gamma < 3$, K exhibits a sublinear growth, which leads to

$$\hat{K}(S) \simeq 2S + a^2 \frac{S_c^2}{2L}\left(\frac{S}{S_c}\right)^{2\gamma-4}, \quad \text{(D3)}$$

where $a \equiv \langle k_{\rm nn}\rangle \Gamma(4-\gamma)/(\gamma-2)$. The ratio of the second term to the first term is proportional to $(S/L)^{2\gamma-5}$, which is much larger than 1 for $2 < \gamma < 5/2$ and much smaller than 1 for $\gamma > 5/2$, since $S \ll L$. Hence, scaling behaviors of $\hat{K}(S)$ in the regime of $S_c \ll S \ll N$ are represented as

$$\hat{K}(S) \simeq \begin{cases} a^2 \frac{S_c^2}{2L} (S/S_c)^{2\gamma-4} & \text{for } \gamma < 5/2, \\ b\, S & \text{for } \gamma = 5/2, \\ 2S & \text{for } \gamma > 5/2, \end{cases} \quad \text{(D4)}$$

where $b = 2 + \langle k\rangle(\pi/3)$.

[1] A. Vespignani, Science **325**, 425 (2009).
[2] M. Barthélemy, Phys. Rep. **499**, 1 (2011).
[3] H. A. Makse, S. Havlin, and H. E. Stanley, Nature **377**, 608 (1995).
[4] G. Krings, F. Calabrese, C. Ratti, and V. D. Blondel, J. Stat. Mech. (2009) L07003.
[5] S. Eubank, H. Guclu, V. S. Anil Kumar, M. V. Marathe, A. Srinivasan, Z. Toroczkai, and N. Wang, Nature **429**, 180 (2004).
[6] G. M. Viswanathan, V. Afanasyev, S. V. Buldyrev, E. J. Murphy, P. A. Prince, and H. E. Stanley, Nature **381**, 413 (1996).
[7] D. W. Sims, E. J. Southall, N. E. Humphries, G. C. Hays, C. J. A. Bradshaw, J. W. Pitchford, A. James, M. Z. Ahmed, A. S. Brierley, M. A. Hindell, D. Morritt, M. K. Musyl, D. Righton, E. L. C. Shepard, V. J. Wearmouth, R. P. Wilson, M. J. Witt, and J. D. Metcalfe, Nature **451**, 1098 (2008).
[8] D. Brockmann, L. Hufnagel, and T. Geisel, Nature **439**, 462 (2006).
[9] M. C. González, C. A. Hidalgo, and A.-L. Barabási, Nature **453**, 779 (2008).
[10] C. Song, Z. Qu, N. Blumm, and A.-L. Barabási, Science **327**, 1018 (2010).
[11] A. Chmiel, K. Kowalska, and J. A. Hołyst, Phys. Rev. E **80**, 066122 (2009).
[12] C. Song, T. Koren, P. Wang, and A.-L. Barabási, Nat. Phys. **6**, 818 (2010).
[13] B. D. Hughes, *Random Walks and Random Environments* (Clarendon Press, Oxford, London, 1995), Vol. 1.
[14] D. Ben-Avraham and S. Havlin, *Diffusion and Reactions in Fractals and Disordered Systems* (Cambridge University Press, Cambridge, 2000).
[15] S. Redner, *A Guide to First-Passage Processes* (Cambridge University Press, Cambridge, 2001).
[16] R. Metzler and J. Klafter, Phys. Rep. **339**, 1 (2000).
[17] J. Park, D.-S. Lee, and M. C. González, J. Stat. Mech. (2010) P11021.
[18] N. Kumar, U. Harbola, and K. Lindenberg, Phys. Rev. E **82**, 021101 (2010).
[19] J. Choi, J.-I. Sohn, K.-I. Goh, and I.-M. Kim, Europhys. Lett. **99**, 50001 (2012).
[20] D. Boyer and C. Solis-Salas, Phys. Rev. Lett. **112**, 240601 (2014).
[21] U. Harbola, N. Kumar, and K. Lindenberg, Phys. Rev. E **90**, 022136 (2014).
[22] M. A. A. da Silva, G. M. Viswanathan, and J. C. Cressoni, Phys. Rev. E **89**, 052110 (2014).
[23] H.-J. Kim, Phys. Rev. E **90**, 012103 (2014).
[24] V. B. Sapozhnikov, J. Phys. A: Math. Gen. **27**, L151 (1994).
[25] F. D. A. A. Reis, J. Phys. A: Math. Gen. **28**, 3851 (1995).
[26] J. W. Lee, J. Phys. A: Math. Gen. **31**, 3929 (1998).
[27] A. Ordemann, G. Berkolaiko, S. Havlin, and A. Bunde, Phys. Rev. E **61**, R1005(R) (2000).
[28] A. Ordemann, E. Tomer, G. Berkolaiko, S. Havlin, and A. Bunde, Phys. Rev. E **64**, 046117 (2001).
[29] J. G. Foster, P. Grassberger, and M. Paczuski, New J. Phys. **11**, 023009 (2009).
[30] E. Agliari, R. Burioni, and G. Uguzzoni, New J. Phys. **14**, 063027 (2012).
[31] A.-L. Barabási and R. Albert, Science **286**, 509 (1999).
[32] R. Albert and A.-L. Barabási, Rev. Mod. Phys. **74**, 47 (2002).
[33] S. Boccaletti, V. Latora, Y. Moreno, M. Chavez, and D.-U. Hwang, Phys. Rep. **424**, 175 (2006).
[34] M. E. J. Newman, *Networks: An Introduction* (Oxford University Press, Oxford, 2010).
[35] A. Barrat, M. Barthelemy, and A. Vespignani, *Dynamical Processes on Complex Networks* (Cambridge University Press, Cambridge, 2008).
[36] L. K. Gallos, Phys. Rev. E **70**, 046116 (2004).
[37] M. Chupeau, O. Bénichou, and R. Voituriez, Nat. Phys. **11**, 844 (2015).
[38] M. Molloy and B. A. Reed, Random Struct. Alg. **6**, 161 (1995).
[39] M. Boguñá, R. Pastor-Satorras, and A. Vespignani, Eur. Phys. J. B **38**, 205 (2004).
[40] J. D. Noh and H. Rieger, Phys. Rev. Lett. **92**, 118701 (2004).
[41] M. E. J. Newman, Phys. Rev. E **67**, 026126 (2003).
[42] C. Song, S. Havlin, and H. A. Makse, Nature **433**, 392 (2005).
[43] C. Song, S. Havlin, and H. A. Makse, Nat. Phys. **2**, 275 (2006).
[44] K.-I. Goh, G. Salvi, B. Kahng, and D. Kim, Phys. Rev. Lett. **96**, 018701 (2006).
[45] J. S. Kim, K.-I. Goh, G. Salvi, E. Oh, B. Kahng, and D. Kim, Phys. Rev. E **75**, 016110 (2007).
[46] J. S. Kim, K.-I. Goh, B. Kahng, and D. Kim, New J. Phys. **9**, 177 (2007).
[47] C. Domb and G. S. Joyce, J. Phys. C **5**, 956 (1972).
[48] H. E. Stanley, K. Kang, S. Redner, and R. L. Blumberg, Phys. Rev. Lett. **51**, 1223 (1983).
[49] D. J. Amit, G. Parisi, and L. Peliti, Phys. Rev. B **27**, 1635 (1983).
[50] P. M. Duxbury, S. L. A. de Queiroz, and R. B. Stinchcombe, J. Phys. A: Math. Gen. **17**, 2113 (1984).
[51] P. M. Duxbury and S. L. A. de Queiroz, J. Phys. A: Math. Gen. **18**, 661 (1985).
[52] H. C. Ottinger, J. Phys. A: Math. Gen. **18**, L363 (1985).
[53] S. N. Dorogovtsev and J. F. F. Mendes, Adv. Phys. **51**, 1079 (2002).
[54] M. Abramowitz and I. A. Stegun, *Handbook of Mathematical Functions: With Formulas, Graphs, and Mathematical Tables* (Dover, New York, 1965).